*Research Article*

http://dx.doi.org/10.21060/cis.2014.231

# Study of a new rare-earth malonate and comparative investigations between oxo-bridged Ce(III) and alkaline-earth Ca(II) and Ba(II) malonates

**Khadidja Aliouane[a], Belkacem Benmerad[a,b], Narimène Rahahlia-Taïeb[a], Hamza Kherfi[a], Achoura Guehria-Laïdoudi [a,*], Slimane Dahaoui[c], Claude Lecomte[c].**

[a] Crystallography-Thermodynamic Laboratory, Faculty of chemistry, USTHB, BP 32, El-Alia, Bab-Ezzouar, Algiers, Algeria. [b]Department of chemistry, Faculty of Sciences, Bejaia University, Algeria. [c]CRM2, UMR-CNRS 7036, Jean Barriol Institut, Lorraine University, BP 230, 54506, Vandoeuvre-Les-Nancy cedex, France.

E-mail : guehria_laidoudi@yahoo.fr

*Received: July 22, 2014; accepted September 20, 2014*

**Abstract:** A new Ce(III)-malonate, growth by hetero-nuclear synthesis, is investigated structurally at 100K. In this oxo-bridged material, the bi-anion does not allow the formation of any synthons, but various bridges form connections displaying typical sub-features. Cross-linked edge-shared $CeO_9$ and $CeO_7(H_2O)_3$ polyhedrons built up 3D packing accommodating two water molecules embedded in extensive H-bonds. Stable at 25° C, it undergoes concomitant dehydration and decarboxylation sequences. By comparison, Ca(II)-hydrogenmalonate and acidic Ba-malonate are also oxo-bridged polymers, but obtained differently and are much more stable. The former shows face-sharing binuclear units, and synthons. The protonated ligands present in the two alkaline-earth materials give peculiar decomposition process.

**Supporting information**: TGA/ DTA/ DTTA curves of Ca-based compound, TGA/ DTA/ DTTA curves of Ba-based compound, Coordination polyhedrons and fragment of 3D framework in Ce-malonate, Cross-linked layers in Ce-malonate, The C(6) synthons in Ca-based compound, The bi-polyhedron stacking in Ca-based compound, Crystal data, collection procedures and refinement for Ce-malonate, Selected geometric parameters in Ce coordination spheres, Hydrogen-bond geometry in Ce-malonate, XRPD(X-ray powder diffraction) patterns of some intermediate and final TG products.

**Keywords**: *Rare-earths; X-Ray crystal structure; Alkaline-earths; Thermal behaviour, H-bonds; Coordination polymers*.

## 1. INTRODUCTION

Rare-earth and alkaline-earth ions share numerous common properties: large ionic radii assuming high coordination numbers, great affinity for O-donor ligands, and low directionality due to their mostly electrostatic binding interactions; such characteristics broaden their field of applications [1, 2]. When these ions are associated with ligands displaying coordination versatility , such as the ligands stemming from aliphatic $\alpha,\omega$-dicarboxylic acids HOOC-$(CH_2)_n$-COOH [$H_2L$], they are used in biological system for their related structural role in binding sites, and in solid state chemistry, as precursors in the synthesis of superconductor oxides and advanced materials [1-6].

In the homo-nuclear approach, our aim is to test the substitution of alkaline-earth ions (M) by rare-earth ions (Ln) and examine the isomorphic possibilities, the identical sub-features and the supra-molecular arrays offered to biochemistry as new incorporated strands [4,7]. From solid-state point of view, the building-block methodology given by lanthanide and/or alkaline-earth metals as connectors (Ln = $La^{3+}$, $Ce^{3+}$; M = $Ba^{2+}$, $Ca^{2+}$) is interesting in hetero-bimetallic complexes that form binuclear basic units. This entity, if subjected to thermal decomposition, can be a soft chemical way for replacing the ceramic method used generally in perovskite-like materials. Unfortunately, we could not achieve hetero-bimetallic complexes such as those which contain transition metals [8, 9]; however, we have obtained mainly homo-metallic compounds. Herein, we present correlative thermal behaviours and specific crystalline features of new rare-earth malonate $\{[Ce_2(C_3H_2O_4)_3(H_2O)]2H_2O\}^3_\infty$ (**1**), obtained by using hetero-nuclear approach, and we compare some results with two alkaline-earth compounds obtained using these two approaches, focusing principally on $\{[Ca(C_3H_3O_4)_2]\}^3_\infty$ (**2**).

## 2. EXPERIMENTAL

All chemicals were high purity from Merck Co. By applying hetero-nuclear synthesis conditions, we have synthesized a new Ce(III) complex which contains the bi-anion [$L^{2-}$]. Under con-

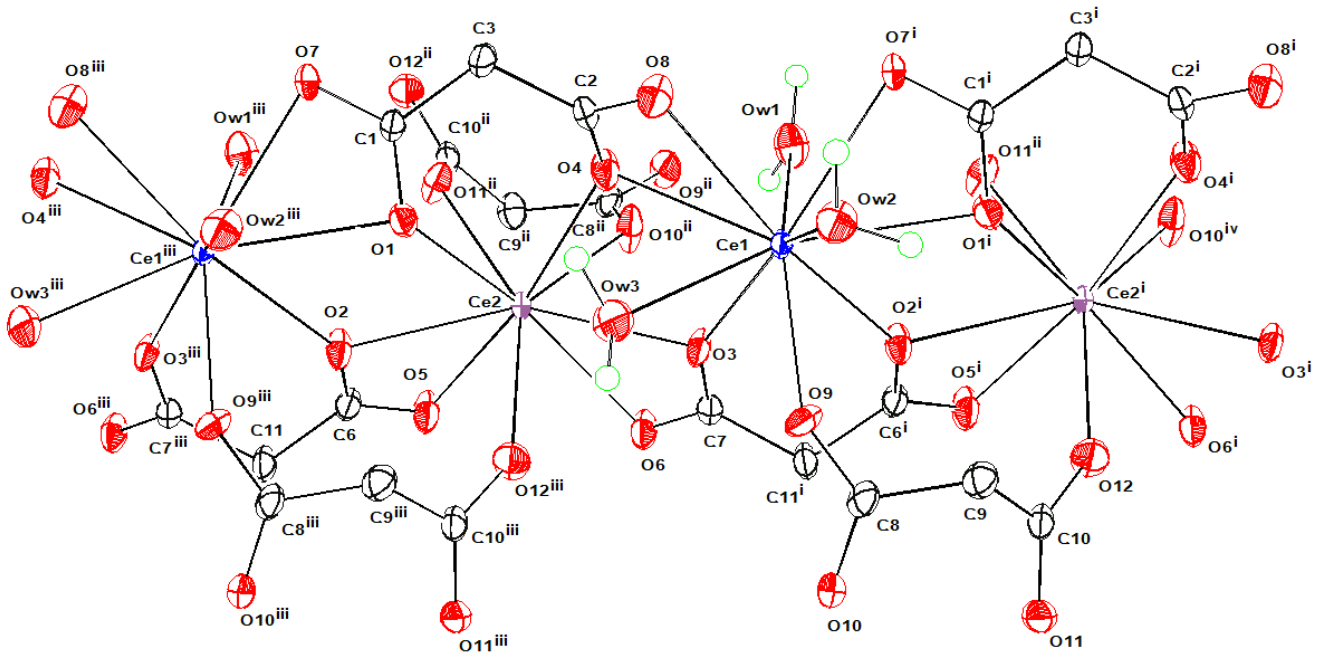


**Figure 1**: The oxo-bridged Ce…Ce chain showing the ligands coordination modes. Symmetry codes: (i) : -1+x y z ; (ii) : 1-x -0.5+y 2-z ; (iii) : 1+x y z ; (iv) : -x -0.5+y 2-z

tinuous stirring, 3 mmol of malonic acid, 1 mmol of Cerium chloride $CeCl_3.7H_2O$, and 1 mmol of Calcium hydroxide, were successively dissolved in 100 mmol deionised water. Always under stirring, a solution of malonic acid (0.6 mmol; 0.0662g in 0.05mL of $H_2O$) was finally added to give a mixture with pH below 4. After three hours, the preparation was filtered and the mother liquor was stored at room temperature. Crystals of homo -metallic Ce-based compound appear in this resulting solution after one month. Yield: 0.1621g, 48% (based on Ce). Anal. Calc.: C, 15.98; H, 2.39. Found: C, 15.54; H, 2.24. In proceeding with the same mixture ratios but using the oxide $La_2O_3$ and the hydroxide $Ba(OH)_2.8H_2O$ for providing metals, then adjusting the pH above 5, we obtained crystals identified, by its preliminary single crystal XRD data, as the structurally known homo-metallic Ba-based compound containing both $[L^{2-}]$and $[H_2L]$ ligands $Ba(L)(H_2L)_2$[10]. Yield: 0.1431g, 32% (based on Ba). Anal. Calc.: C, 24.15; H, 2.25. Found: C, 23.78; H, 2.18. X-Ray single crystal data collection was performed on a Kappa-CCD diffractometer at 100(2) K. Empirical absorption corrections were applied by using MULABS in PLATON programs [11]. Thermal gravimetric (TGA) and differential thermal analyses (DTA and DTTA) were conducted simultaneously on powdered samples using SETARAM 92-16 equipment; the heating rate was 4°C.min$^{-1}$ in air from ambient to 400°C for Ca-hydrogenmalonate (Figure S1) and to 800°C for acidic Ba-malonate (Figure S2) and Ce-malonate. For studying TG products, XRPD (X-ray powder diffraction) patterns were obtained on an expert pro analytical MPd equipped with CuKα radiation in the range $5° < \theta < 70°$ with a step size of 0.02° (2θ) and a count time of 2s per step. The crystal structure of **(1)** was solved by direct methods and subsequent Fourier analysis, then refined by full-matrix least squares using 5053 reflections (I > 2s (I)), with anisotropic thermal parameters for all non-hydrogen atoms. All H atoms were located in a difference-Fourier map and methylene H-atoms were treated as riding, with C-H = 0.99 Å and $U_{iso}(H) = 1.2U_{eq}(C)$. Unlike one isotypic Pr(III) compound [12], H-atoms of the five water molecules were found, then refined with restraints. The programs SHELXS and SHELXL [13] with WinGX environment [14] were used for computations. Peak and hole are respectively 0.82Å from Ce1, 0.87Å from Ce2. Crystal data, collection procedures and refinement results are summarized in Table S1. We have already reported those of (**2**) [15]. $\{[Ca(C_3H_3O_4)_2]\}^3_\infty$ has been obtained by homo-nuclear approach. Yield: 0.1284g, 52% (based on Ca). Anal. Calc.: C, 29.19; H, 2.45. Found: C, 29.95; H, 2.63.

## 3. RESULTS AND DISCUSSION

In the hetero-nuclear approach, with the simplest ligands (n=0, 1) stemming from a,w aliphatic dicarboxylic acids, conventional synthetic route under room temperature and hydrothermal method are currently used. They allowed single crystal's growth of hetero-bimetallic compounds, essentially when the starting materials are salts, and in the case of transition metals mixed with alkaline or alkaline-earth metals [6, 8, 9]. When the connectors are oxides or hydroxides, and with f, d or s block's metals, one obtains supra-molecular homo-metallic materials, as for the Ba-based material, and (**2**).It seems that the number of aqua ligands [4] affects the assembly process contrary to the temperature of

synthesis. Moreover, the pH value plays probably the major role in the acid's deprotonation and single crystal's growth [4, 10]. Despite their different charges and ligands, Ce(III)-based, Ca(II) -based, and Ba(II)-based [10] compounds are built up from units containing oxo-bridges. In **(1),** each crystallographically different metal is connected to two neighbouring ones, through four $m_2$-oxo bridges, to form repeat four-membered Ce/O/Ce/O rings and infinite metal-metal chain running in zig-zag manner (Figure 1).

As indicated in Table S2, Ce-O bonds reveal some dispersion, and confirm the different geometries around each metal. The geometry around Ce1 is intermediate between a bi-capped (O2W and O3W), dodecahedron and a bi-capped ($O7^{i}$ and $O3^{i}$), square prism (Figure S3). The mono-capped square antiprism formed around Ce2, is also distorted, the two square planes are formed respectively by $O10^{ii}$, $O11^{ii}$, O2, $O6^{i}$ and $O3^{i}$, O4, O1, $O12^{iii}$. The atom O5 appears as an axial cap (Figure S3). Within the infinite puckered diamond-shaped rings, the distances between successive $Ce^{3+}$ ions are almost equal: 4.4790(49)Å (connection across O2 and O1) and 4.2435(59)Å (connection across O3 and O4). Table 1 presents selected bond lengths and angles of the three independent ligands. They all display malonate mode. Those having six ligating atoms (L1 and L2) play the similar role in:

(i) bridging metal atoms through their double $\mu_2$-O′;$k^2$ O,O′ bridges.

(ii)bringing out infinite chains where it appears the M-O-M-O typical connectivity encountered in MOFs (Figure 1). They involve their four O-donor atoms to form two-dimensional polymeric carboxylate layers (Figure S4). Moreover, adjacent chains are linked together through $\mu_2$-carboxylato-$k^1$:$k^1$O′ bridges of the third ligand (L3), leading to a 3D packing (Figure S4).

The three ligands present multiple bridging modes leading to the "Poly[[triaquabis($\mu_3$-malonato-$k^6O^1,O^3:O^{1'}:O^{1'},O^{3'}:O^{3'}$)($\mu_3$-malonato-$k^4O^1:O^{1'},O^{3'}:O^{3'}$) dicerium (III)] dihydrate]" (Table 1). L1 and L2 involve their two end functional groups in different conformations: one is *syn-anti* (the angles deviate significantly from 60° and 180° ideal values) and the other is *anti-anti*, the corresponding torsion angles being very close to 180° (Table 1). The two end functional groups of L3 are in *syn-syn* conformation, with corresponding torsion angles near the ideal value.

Despite its unique ligand, Ca-based compound **(2)** shows also multiple bridges ($\mu_2$-O′; $k^2$O,O′oxo and $\mu_2$-$k^1$O:$k^1$O′carboxylato) associated to malonate mode, leading to "Poly[bis($\mu_3$-hydrogenmalonato-$k^4O^1,O^3:O^{1'},O^{3'}$) Calcium(II)]" where infinite C(6) synthons, are in *syn-syn* conformation (Figure S5). These head- to-tail hydrogen bonds give rise to another cage-like assembly involving four such strong interactions provided by eight ligands. Therefore, these intermolecular bindings explain the crystalline stability, despite the wide empty channels surrounded by the helical stacking of the bi-polyhedron and the carbon backbone of the ligands (Figure S5 and Figure S6). On the contrary, Ce-based compound contains, between its layers, two guest water molecules stabilized by hydrogen bonds which participate in the overall 3D MOF (Figure S3). The extensive H -bonds network (Table S3) shows bifurcated and medium to strong bonds between [$L^{2-}$] and aqua ligands and between water molecules themselves. In other lanthanide malonates known, one Pr(III) malonate[12] is isotypic with **(1)**, and two La (III)-based compounds have the same empirical formula $La_2(C_3H_2O_4)_3.5H_2O$ [16, 17], but one is tetraaqua complex [16], while the second has an almost identical chemical formula [17] to **(1)**. Examination of its structure shows that the two overall frameworks are closely related. However, the two independent La (III) display the same ten-coordination implying each aqua ligands. Moreover, the third ligand, is three times mono-dentate and without malonate mode.

This new Ce(III) compound begins losing weight directly upon starting the thermal experiments (Figure 2).Two consecutive processes, up to 240°C, lead respectively to 14.36% and 5.04% weight losses which are consistent with the release of 5 $H_2O$

**Table 1**: Selected geometric parameters (Å; °) in the three independent ligands.

| Ligand L1 | | Ligand L2 | | Ligand L3 | |
|---|---|---|---|---|---|
| O3–C7 | 1.262(9) | O1–C1 | 1.258(10) | O11–C10 | 1.247(10) |
| O6–C7 | 1.246(9) | O7–C1 | 1.258(9) | O12–C10 | 1.264(11) |
| $C7^{i}$–C11 | 1.522(11) | C1–C3 | 1.512(11) | C10–C9 | 1.517(11) |
| C11–C6 | 1.523(10) | C3–C2 | 1.501(11) | C9–C8 | 1.523(12) |
| O2–C6 | 1.262(9) | O4–C2 | 1.261(10) | O9–C8 | 1.253(10) |
| O5–C6 | 1.256(9) | O8–C2 | 1.266(10) | O10–C8 | 1.247(11) |
| O3–C7–C11–C6 | -36.106(11) | O1–C1–C3–C2 | 11.0(14) | O11–C10–C9–C8 | 64.1(9) |
| O6–C7–C11–C6 | 145.671(8) | O7–C1–C3–C2 | -170.6(9) | O12–C10–C9–C8 | 116.4(8) |
| O2–C6–C11–$C7^{ii}$ | -140.6(9) | O4–C2–C3–C1 | 41.3(14) | O9–C8–C9–C10 | 122.0(8) |
| O5–C6–C11–$C7^{ii}$ | 40.2(13) | O8–C2–C3–C1 | -140.7(9) | O10–C8–C9–C10 | 58.3(11) |

Symmetry codes: (i): 1+x y z; (ii): -1+x y z

and 1 $CO_2$ per formula unit (calc: 19.95% ; exp: 19.40%). These events are reflected on DTA curve by two endothermic peaks centred at 115.2°C and 241.3°C. In Pr-malonate, the two first stages correspond to the release of water molecules only [12].

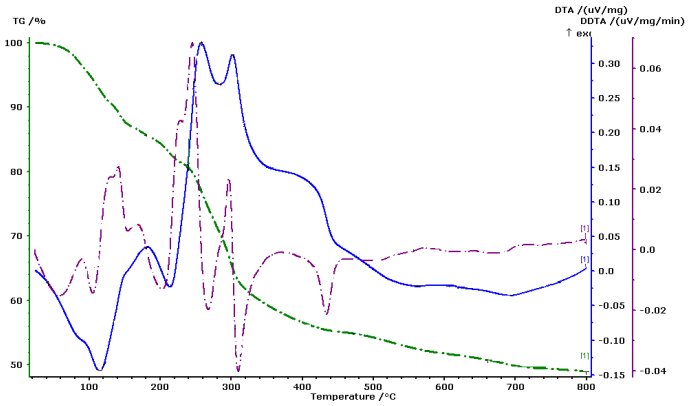


**Figure 2.** TGA, DTA, DTTA curves of Ce-malonate

In **(1)**, the departure of all water molecules whatever they are, coordinate or uncoordinate, and the starting, in the same time, of the decarboxylation of one ligand are supported by our structural results. Thus, as shown in Table S2, $Ce_1$-O (aqua ligands) bonds are stronger than $Ce_1$-O (carboxylate ligands) bonds. Elsewhere, in Table S3, it appears that the strongest H-bond implies one oxygen of L2 (O8), which is at the centre of two H-bonds provided by one aqua ligand (O2W) and one solvent molecule (O5W). The intermediate product is not stable, as three further successive losses of 25.82%, 4.07%, and 1.78%, are accompanied respectively by two exothermic peaks (258.4°C and 302.5°C) and two endothermic peaks (562.6°C and 692.8° C). During these steps, the formation of one complex product [18], doesn't match with the experimental data. Whereas the oxycarbonate $Ce_2O_2CO_3$ is probably formed after the three first stages (% exp Δm of 54.78 approximates the % calc value of 55.03). The XRPD of the white compound obtained at 460°C shows that this intermediate product doesn't contain any calcinations product and has good crystal quality (Figure S7). Above 474°C, and during the two last sequences, the decomposition of $Ce_2O_2CO_3$ to give $Ce_2O_3$, after the release of 1 $CO_2$ per formula unit (exp Δm : 5.85%; calc Δm calc: 6.65%), is in agreement with the remained weight of 48.93% in final homogeneous white residue (calc 48.52%),(Figure S8), and with the stability's temperature range of Ln oxycarbonates [19].

In **(2),** the decarboxylation starts at a lower temperature (122° C), (Figure S1) if compared to Ba-based compound that we have obtained in using hetero-nuclear approach (148°C) (Figure S2). This event occurs for **(2)** in two successive steps, up to 228°C, corresponding to the release of 5CO and 1 $H_2O$ per formula unit (exp 64.68%; calc 64.16%), and it is associated to three endothermic peaks (134.2; 159.7; 203.9)° C. Whereas in Ba(II)-based compound, a strong endothermic peak starts with the beginning of weight loss. Centred at 197.7°C, during the first TG stage (148-266)°C, it can be ascribed to the departure of 5CO and 4 $H_2O$ per formula unit (% exp Δm: 47.54; % calc Δm 47.68). The intermediate product is subjected immediately to two consecutive steps, leading probably to BaO with pyrolysis C residue, after the release of 1 $CO_2$ per formula unit (% exp: 9.66; % calc: 9.89). This is confirmed by XRPD of final black mixed amorphous residue (Figure S9). Concerning **(2)**, it is most reasonable to excluded $CaCO_3$ as intermediate product for it, the experimental mass of 35.32% is much lower than the corresponding theoretical mass for $CaCO_3$ (40.61%). None of the products appearing in the decomposition of transition and alkaline-earth malonates, matches with the experimental value found [20]. Its composition corresponds to a probable $Ca(OH)_2$ beside carbon pyrolysis residue. This product loses $1H_2O$ (% exp: 7.74; % calc: 7.31), during the two last stages to give a final black mixed amorphous residue containing CaO (% exp for the remained residue: 27.48; % calc with C pyrolysis residue: 27.27) (Figure S10). Likewise, the numerous endothermic peaks, occurring in all weight losses steps, as well as during the plateau, may be interpreted as reflecting possible atomic rearrangements [20] during the two first steps. It is evidenced here that the thermal behaviour of **(2)** is much more comparable to the anhydrous $Ba(L)(H_2L)_2$.

**Acknowledgments**

The authors would like to express their thanks to MESRS-Algeria and MDU-France, for financial support (project CMEP-Programme Tassili) and are grateful to Pr. T. Abadlia and D. Aouanouh of Boumerdes University, Algeria, for TGA/DTA measurements.

**Supplementary Material**

X-Ray crystallographic files for the Ce-malonate and Ca-hydrogenmalonate on CIF format are available free of charge via Internet at http://pubs.acs.org. CCDC n°739498 for compound **(1)** and Acta Cryst. E63, m1834 (2007) for compound **(2)**.

**REFERENCES**

[1] Allendorf, M.D.; Bauer, C.A.; Bhakta, R.K. and Houk, R.J.T. *Chem. Soc. Rev.* **2009,** 38,1330.

[2] Li, L.; Liao, D.; Jiang, Z. and Yan, S. *Inorg. Chem.* **2002**,

41, 421.

[3] Zell, A.; H. Einspahr, H. and Bugg, C.E. *Biochemistry* **1985**, 24, 533.

[4] Chrysomallidou, K.E.; Perlepes, S.P.; Terzis, A. and Raptopoulou, C.P. *Polyhedron* **2010**, 29, 3118.

[5] Jung, W.S.; Lee, T. J. and Min, B. K. *Mater. Lett.* **2003**, 57, 4237.

[6] Gil de Muro, I.; Mautner, F.A.; Insausti, M.; Lezama, L.; Arriortua, M.I. and Rojo, T. *Inorg. Chem.* **1998**, 37, 3243.

[7] Rühl, T. and Stulz, E. *Supramol. Chem.* **2010**, 22, 103.

[8] Djeghri, A.; Balegroune, F.; Guehria-Laïdoudi, A. and Toupet, L. *J. of Chem. Crystallogr.* **2005**, 35, 603.

[9] Kherfi, H.; Hamadène, M.; Guehria-Laidoudi, A.; Dahaoui, S. and Lecomte, C. *Acta Cryst.* **2011**, C67, m85.

[10] Hodgson, D. J. and R. O. Asplund, R. O. *Inorg. Chem.* 30, **1991**,18, 3577.

[11] Spek, A.L. *Acta Cryst.* **2009**, D65, 148.

[12] Hernandez-Molina, M.; Lorenzo-Luis, P.A.; Lopez, T.; Ruiz-Perez, C.; F. Lloret, F.and Julve, M. *CrystEngComm.* **2000**, 2,169.

[13] Sheldrick, G.M. *Acta Cryst.* **2008**, A64,112.

[14] Farrugia, L.J. *J. Appl. Cryst.* **1999**, 32, 837.

[15] Aliouane, K.; Rahahlia, N.; Guehria-Laïdoudi, A.; Dahaoui, S. and Lecomte, C. *Acta Cryst.* **2007**, E63, m1834.

[16] Benmerad, B.; Guehria-Laïdoudi, A.; Bernardinelli, G. and Balegroune, C. *Acta Cryst.* **2000**, C56, 321.

[17] Marrot, F. and Trombe, J.C. *C. R. Acad. Sci.* **1993**, 317, 319.

[18] Muraishi, K.; Suzuki, Y. and Takahashi, Y.*Thermochimica Acta* **1996**, 286, 187.

[19] Doreswamy, B.H. ; Mahendra, M.; Sridhar, M. A. ; Prasad, J. S.; Varughese, P. A.; Saban, K. V. and Varghese, G. *J. Mol. Struct.* **2003**, 659, 81.

[20] Muraishi, K.; Nagase, K.; Kirughi, M.; Sone, K. and Tanaka, N. *Bull. Chem. Soc. Jpn.* **1982**, 66, 1645.

*This is an open access article distributed under the Creative Commons Attribution License, which permits unrestricted use, distribution, and reproduction in any medium, provided the original work is properly cited.*